Lab on a Chip

Accepted Manuscript

ROYAL SOCIETY OF CHEMISTRY

www.rsc.org/loc

Table of Contents Figure

Massively size-reduced, phase changeable, monodisperse perfluorocarbon (PFC) nanodroplets were generated for ultrasound medical imaging using condensation and dissolution of microfluidic-generated, cosolvent-incorporated PFC bubbles.

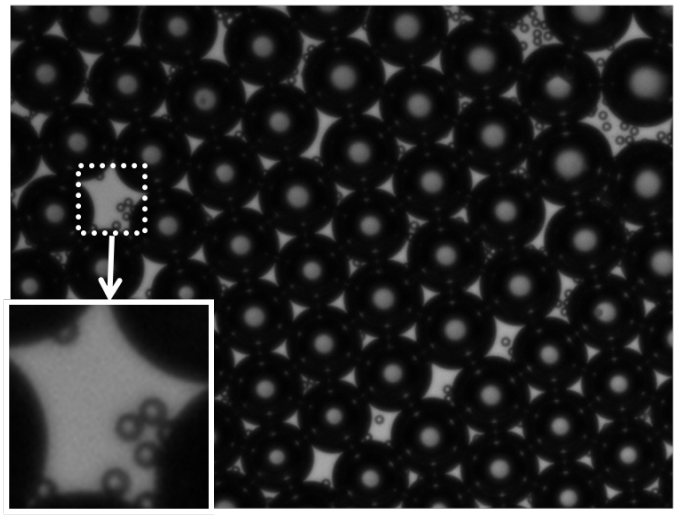

1/23

Size Reduction of Cosolvent-Infused Microbubbles to Form Acoustically Responsive Monodisperse Perfluorocarbon Nanodroplets†

Minseok Seo[1], Ross Williams[1], and Naomi Matsuura[2, 3]*

[1]Physical Sciences, Sunnybrook Research Institute
2075 Bayview Avenue, Toronto, ON, M4N 3M5, Canada
[2]Department of Medical Imaging, University of Toronto
[3]Department of Materials Science and Engineering, University of Toronto
263 McCaul St., Toronto, ON, M5T 1W7, Canada
*E-mail: matsuura@sri.utoronto.ca

Keywords: Fluorocarbon, Nanoparticle, Condensation, Dissolution, Microfluidics, Medical Imaging

†Electronic Supplementary Information (ESI) available: Determination of diethyl ether (DEE) volume expansion coefficient from liquid to gas phase; and a movie of nanoscale perfluorocarbon (PFC) droplets imaged using low-power ultrasound before, during, and after their conversion to bubbles. See DOI: 10.1039/b000000x/

Abstract

Perfluorocarbon (PFC) nanodroplet agents are exciting new biomaterials that can be remotely vapourized by ultrasound or light to change into micron-scale gas bubbles *in situ*. After PFC nanodroplet vapourization, the micron-scale gas bubble can interact strongly with ultrasound radiation, such that the bubbles can be used for cancer imaging and therapy. For these phase-change agents to be useful, however, PFC nanodroplets must be produced in the range of 100 to 400 nm in diameter with high size control and monodispersity, restrictions that remain a challenge. Here, we address this challenge by taking advantage of the size control offered by microfluidics, in combination with the

size reduction provided by cosolvent-infused PFC bubbles through both condensation and cosolvent dissolution. In this approach, PFC bubbles with a high percentage of cosolvent (in this study, diethyl ether, DEE) are produced using microfluidics at a temperature above the boiling point. After synthesis, these bubbles become much smaller through both condensation of the gas into liquid droplets and from dissolution of the DEE into the continuous phase. This approach demonstrates that monodisperse, cosolvent-incorporated PFC bubbles can directly form monodisperse PFC nanodroplets a factor of 24 times smaller than the precursor bubbles. We also demonstrate that these nanoscale droplets can be converted to echogenic microbubbles after exposure to ultrasound, showing that these PFC nanodroplets are viable for the *in situ* production of ultrasound contrast agents. We show that this system can overcome the minimum droplet size limit of standard microfluidics, and is a powerful new tool for generating monodisperse, PFC phase-change ultrasound contrast agents for treating and imaging cancer.

Introduction

Perfluorocarbon (PFC) nanodroplets represent a powerful new paradigm in which a single agent can be remotely activated *in situ* for both cancer imaging and therapy. PFC nanodroplets (~ 100 to ~ 400 nm) are biocompatible, injectable agents with a long history in biomedicine as contrast agents and artificial oxygen carriers.[1, 2] Recently, PFC nanodroplets have been proposed as unique phase-change agents that can be converted *in situ* by light or ultrasound from nanoscale liquid droplets to micron-scale bubbles. These phase-change agents have two properties that make them promising for cancer imaging and therapy. First, the size of the liquid nanoscale droplets permits their accumulation in disease sites not accessible to the larger echogenic bubbles (e.g., within solid tumours)[3, 4] where local medical imaging and therapy are highly desirable. Second, these small liquid-phase PFC agents interact weakly with diagnostic ultrasound frequencies and are inefficient ultrasound imaging and therapy agents; however, post-conversion, the nanoscale phase-change droplets expand to become echogenic micron-scale gas bubbles 1 to 8 μm in diameter that resonate nonlinearly with ultrasound waves at diagnostic frequencies and are ideal for use in ultrasound imaging or treatment.

In addition to the well-known size-dependent biological properties of nanoscale agents,[5, 6] the energy required to convert nanoscale droplets to micron-scale bubbles is also strongly dependent on the size of the droplets.[7] The ability to tightly control the size distribution of the PFC nanodroplets is the next barrier that must be overcome for effective and controlled PFC nanodroplet activation to better enable the use of these agents in cancer imaging and therapy *in vivo*. Current microfluidic techniques have the ability to produce emulsions with excellent size control and with exceptional monodispersity compared to other emulsion synthesis methods, such as agitation, extrusion, and sonication.[8] However, the formation of 'ultra-small' PFC droplets on the scale smaller than a few micrometers is more challenging, since these are substantially smaller than the minimum dimensions of standard microfluidic devices (MFDs).

Microfluidic approaches have been developed to directly produce ultra-small, monodisperse droplets; however, each has its own limitations. For example, the direct generation of droplets in the tip-streaming regime using MFDs produced perfluoropentane (C_5F_{12}) droplets with diameters of 360 ± 50 nm.[9] But, tip-streaming occurs in a narrow capillary number (*Ca*) range of $0.4 < Ca < 1.0$,[10] which requires a very stable, non-fluctuating flows of both the dispersed and continuous phases. Tip-streaming is thus limited to the smallest size of the droplets that can be obtained by changing the dimensions and geometries of the channels and the properties and flow rates of the fluids, with the minimum size determined by the viscous forces and surface/interfacial tensions in the system.[9-11]

Other microfluidic methods for producing ultra-small PFC droplets are indirect. For example, the technique of cosolvent dissolution from cosolvent-infused PFC droplets produced by MFDs has been used to produce size-reduced nanoparticle-incorporated droplets approximately 5 times smaller in diameter than the original droplet.[12] Recently, a new indirect method to produce monodisperse, ultra-small PFC droplets was introduced, which used the condensation of precursor bubbles generated using a MFD operating at temperatures higher than the boiling point (b.p.) of the droplet material.[13] Since the condensation of bubbles is limited by the density difference between the gas and liquid phases of the droplet material, this technique is limited to the formation of final droplets that are ~ 5 times smaller than the precursor PFC bubbles.[13, 14]

Here, we demonstrate a method to combine the condensation and dissolution of cosolvent-infused bubbles generated by MFDs to enable the production of monodisperse PFC droplets substantially smaller in diameter than that which can be achieved using either the condensation or dissolution process alone (Figure 1). The process of nanoscale PFC droplet formation began with bubble formation in the MFD at a temperature above the b.p. of the dispersed mixture. After bubble generation, the mixture cooled and the vapour condensed into a liquid, resulting in a size reduction corresponding to the density difference between the initial vapour phase and the final liquid phase of the mixture. Simultaneously, the cosolvent dissolved from the cosolvent-infused PFC bubble into the surrounding aqueous phase, resulting in a size reduction associated with the initial volume fraction of the cosolvent in the PFC-cosolvent mixture. The combination of condensation and cosolvent dissolution can result in a final PFC droplet size that is significantly smaller in diameter than achievable by standard MFD droplet generation and around five times smaller than a PFC droplet formed using either the condensation or cosolvent dissolution processes alone.[12-14]

We first describe the conditions required to produce monodisperse, cosolvent-infused PFC precursor bubbles using a MFD. Perfluoropentane (C_5F_{12}, with a b.p. of 29.2 °C) was used as the droplet material due to its previous application as a phase-change agent for microbubble formation,[15] while a higher b.p. PFC, perfluorohexane (C_6F_{14}, with a b.p. of 57.2 °C), which is more stable at ambient temperatures,[7, 16] was used for the detailed characterization of the droplet formation process. Next, we discuss the size reduction due to the combined effects of the condensation of the PFC gas and the dissolution of the cosolvent from the bubbles as a function of the PFC concentration in the initial mixture. Finally, we show that the PFC nanoscale droplets formed using this new method are viable as *in situ* precursors for highly size-controlled and echogenic monodisperse microbubbles for ultrasound imaging and therapy. These nanoscale PFC droplets were converted to microbubbles using a medical ultrasound system and validated by optical microscopy and ultrasound imaging.

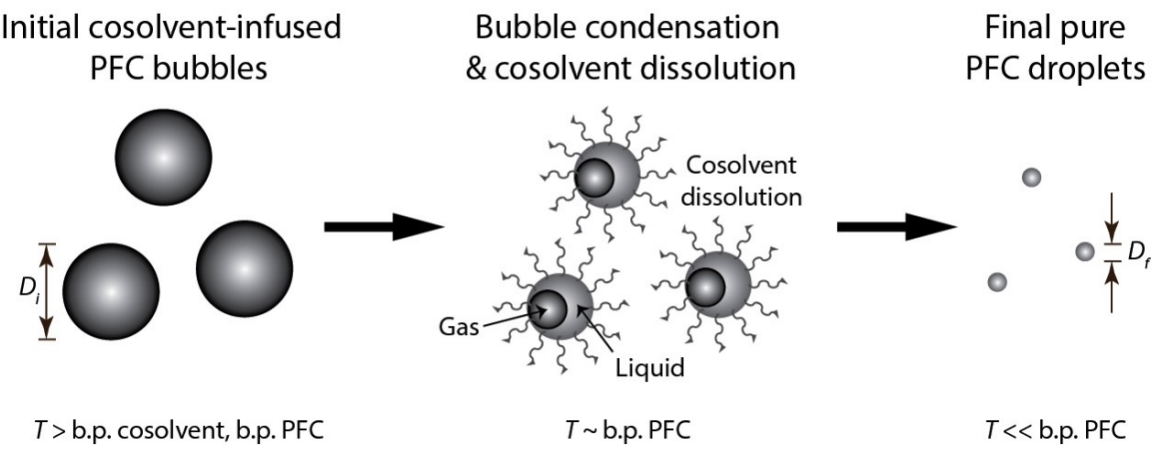

Figure 1. Size-reduced monodisperse PFC droplet formation. Monodisperse cosolvent-infused PFC bubbles of initial diameter D_i are generated in microfluidic devices at a temperature T higher than both the b.p. of the cosolvent and PFC. As the droplet cools below its components' b.p.s, the PFC gas condenses forming a droplet, while the cosolvent condenses and dissolves into the surrounding aqueous phase. After full bubble condensation and cosolvent dissolution, pure, monodisperse PFC droplets with final droplet diameter D_f are formed.

Materials and Methods

Materials:

Zonyl® FSP fluorosurfactant (FSP), pluronic® F-68 (F-68), glycerol, polyvinyl alcohol (PVA), bis acrylamide, citric acid, sodium citrate tribasic dehydrate, L-ascorbic acid, iron (II) sulfate heptahydrate, and 30 % hydrogen peroxide were purchased from Sigma-Aldrich (ON, Canada). The 40 % acrylamide solution in water was purchased from Fisher Scientific (ON, Canada). Deionized water (Millipore Milli-Q grade) with a resistivity of 18.2 MΩ was used in all experiments. Poly(dimethylsiloxane) (PDMS, Sylgard® 184) was purchased from Dow Corning (MI, USA), and photoresist resin (SU-8 25/50 series) was purchased from Microchem Co. (MA, USA). Perfluoropentane (C_5F_{12}, b.p.: 29.2 °C) and perfluorohexane (C_6F_{14}, and b.p.: 57.2 °C) were purchased from FluoroMed, L.P. (TX, USA). All chemicals were used as received.

Methods:

Fabrication of PDMS MFDs: The photomask design process, the microchannel dimensions, the wafer mask patterning, and the PDMS MFD fabrication have been previously described.[13] Briefly, MFDs were designed with typical 3-inlet flow-focusing geometries to form droplets and bubbles of different sizes and with narrow size distributions (Figure 2). Photomasks were designed, transferred to a graphic software (Autodesk Inc., CA, USA), and printed on transparencies with 20,000 dpi resolution (CAD/Art Services, CA, USA). Photolithographic masters with SU-8 25/50 photoresist were prepared using the photomasks on silicon wafers in a Class 10 (ISO Class 4) and Class 1000 (ISO Class 6) clean room facility (University of Toronto, ON, Canada), and soft lithography was used to prepare the PDMS elastomer.[17] Glass slides (75 × 50 mm, and thickness 1.0 mm) were used as the bottom substrates of the MFDs to enhance the thermal conductivity between the heater and PDMS MFD while retaining hydrophilicity. A small amount of thermal paste was used to enhance the thermal conductivity between the heater and bottom glass slide. The heights of the MFD channels were 25 and 95 μm.

In general, the bubbles generated at different flow rates of the continuous and dispersed phases could not fully condense during cooling inside the relatively short length of the MFD outlet channel (30 mm) due to the presence of fluorosurfactant (FSP) and organic surfactant (F-68), that provides a resistance to both PFC condensation and vapourization, inside of the continuous phase as well as the latent heat of condensation of PFCs.[13, 18] Therefore, a tube (0.5 to 1.0 m in length with inner diameter of 0.81 mm) was attached to the MFD immersed in an ice bath to enhance the speed of the condensation (Figure 2).

Hydrophilic surface modification of PDMS MFD: The PDMS MFD microchannels were made hydrophilic using a two-stage process. First, the surface of hydrophobic PDMS was modified by oxygen plasma treatment. Second, the surface of the microchannel was coated with 1 wt. % PVA solution and heat treated to enhance the affinity of the continuous phase to the microchannels.[19]

Generation of precursor bubbles: Three-inlet flow-focusing MFDs were used to generate precursor droplets and bubbles of different sizes and with narrow size distributions. The condensation and dissolution of diethyl ether (DEE) and PFCs were optically quantified using precursor bubbles and droplets with relatively large mean

diameters (D_m > *ca.* 70 μm), generated using an MFD with an orifice width of 50 μm and a channel height of 95 μm (Figure 2b and 2c). Smaller precursor bubbles (D_m < *ca.* 30 μm) for the production of nanoscale PFC droplets were generated using MFDs with an orifice width of 6 μm and a channel height of 25 μm (Figure 2d)). The flow rates of the continuous phase (Q_c) and dispersed phase (Q_d) for both MFD systems were varied from 0.1 to 10.0 and 0.01 to 0.2 mL/h, respectively. DEE-infused PFCs were heated above their b.p. inside of the MFD before the orifice at 45 ± 0.5 °C for DEE-infused C_5F_{12} and 80 ± 0.5 °C for DEE-infused C_6F_{14} using a thermoelectric heater located at the bottom of the glass slide.[13] Mechanical syringe pumps (PHD Ultra Syringe Pumps, Harvard Apparatus, MA, USA) were used to push the continuous and dispersed phases into the microfluidic channels. The continuous phase (0.5 wt. % FSP and 1 wt. % F-68 in 40 ~ 60 wt. % glycerol mixture) was supplied to the two side channels of the MFD, and the dispersed phase (DEE-infused C_5F_{12} or DEE-infused C_6F_{14}) was introduced in the central channel. Fluorosurfactants were selected for emulsification as they have excellent surfactant properties for PFCs, and are also very efficient as their critical micellar concentration (cmc) is commonly two orders of magnitude lower than for similar hydrocarbon-based surfactants. For all experiments, the ambient temperature was maintained at 19.0 ± 0.5°C. No significant changes in the MFD dimensions were observed in any of the experiments due to the high content of the glycerol in the aqueous phase.

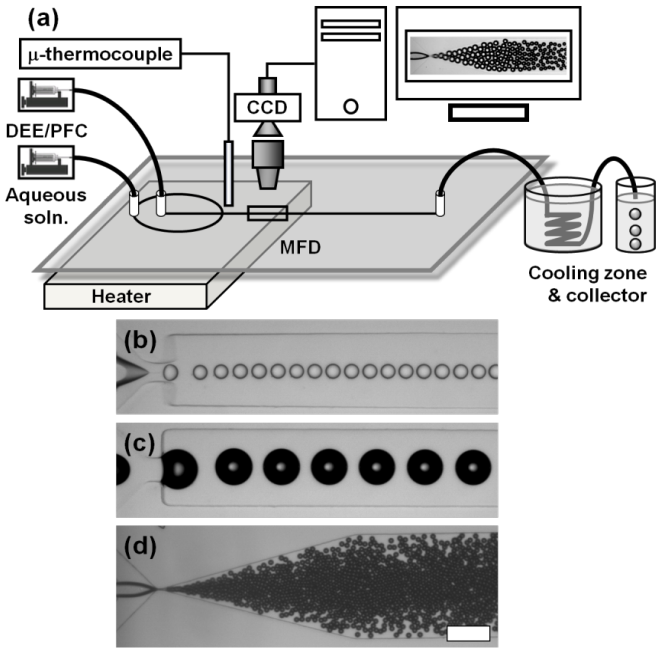

Figure 2. (a) Schematic of the MFD configuration used to generate DEE-infused PFC bubbles and droplets. The MFD dimensions were selected depending on the sizes of the droplets and bubbles required. Microscope images of: (b) 36.6 μm (*CV* = 1.6%) DEE-infused PFC droplets formed at room temperature; (c) 88.8 μm (*CV* = 1.4%) DEE-infused PFC bubbles formed at 80 °C; and (d) 11.6 μm (*CV* = 2.5%) DEE-infused PFC bubbles formed at 80 °C for formation of nanoscale PFC droplets. The MFD orifice widths and heights for (b) and (c) were 50 and 95μm, and for (d) were 6 and 25 μm, respectively. The scale bar represents 100 μm.

Conversion of nanoscale droplets to microbubbles using ultrasound:

Ultrasound experiments were performed using a VisualSonics Vevo2100 ultrasound system (ON, Canada) with 21 MHz-centre-frequency linear array probe (MS-250). Approximately 4×10^5 C_5F_{12} droplets were imbedded into 12 mL of 7 % polyacrylamide (PAA) gel loaded in an OptiCell® cell culture system (Thermoscientific Inc., MA, USA).[15, 20] The probe was positioned perpendicular to the Opticell® chamber containing the droplets in PAA gel, which was immersed in a water bath heated to physiological temperature. All imaging was performed using the nonlinear contrast-specific detection mode operating at 18 MHz, using single-cycle ultrasound bursts. Samples were imaged at low-power (i.e., 800 kPa peak-negative pressure) to visualize the

droplets without inducing vaporization, then exposed to 30 consecutive bursts with peak-negative pressures of 5.0 MPa over a duration of 1 s to convert the droplets into bubbles. The resulting bubbles were imaged again at low power.

Size characterization of generated precursor droplets/bubbles and final PFC droplets: A Leica DMIL inverted microscope system equipped with a high-speed CCD camera (CoolSNAP HQ2, Photometrics, AZ, USA) was used to image bubbles and droplets. Image Pro Plus (Media Cybernetics®, MD, USA) software was used to determine the dimension and the polydispersity (coefficient of variation, *CV*, defined as the standard deviation in droplet/bubble diameter divided by its mean diameter x 100) of the precursor bubbles, precursor droplets, final droplets after condensation and/or dissolution, and vapourized droplets after exposure to ultrasound. For droplets smaller than 1 μm, dynamic light scattering (DLS) was used to measure final condensed droplet sizes, due to the resolution limits of optical microscopy. A Malvern Zetasizer Nano-ZS 3000HS (Worcestershire, UK) dynamic light scattering (DLS) instrument was used to measure the mean diameters of nanoscale droplets. The polydispersity index, PDI, is a measure of the distribution of droplet sizes determined by DLS and is defined as the square of the standard deviation of droplet diameters divided by the square of the mean droplet diameter. PDI values smaller than ~ 0.04 are generally considered monodisperse.[21]

Results and Discussion

1. Generation of monodisperse, DEE-infused PFC precursor bubbles

The formation of monodisperse, diethyl ether (DEE)-infused precursor bubbles at the MFD orifice was accomplished by increasing the MFD orifice temperature (T_o) to 45 °C, above the b.p. of both DEE (34.6 °C) and C_5F_{12} (29.3 °C), and 80 °C, above the b.p. of both DEE and C_6F_{14} (57.2 °C). The effect of varying flow rates (Q_c and Q_d) on the initial diameter (D_i) of the DEE-infused C_5F_{12} precursor bubbles was evaluated (Figure 3a). To maximize the size reduction due to DEE dissolution from the precursor bubble, the bubbles were generated using low concentrations of C_5F_{12} (i.e., volume fractions of $\phi_{C5F12} = 0.015$ and $\phi_{DEE} = 0.985$). Figure 3 (a) shows that the DEE-infused C_5F_{12} bubble size decreased with increasing Q_c for a fixed Q_d. These conditions produced DEE-infused

C_5F_{12} bubbles with sizes ranging from 4.3 to 18.9 μm and with *CV*s ranging from 2 to 4 % in the flow-focusing regimes, at production rates of ~3 x 10^9 bubbles/min to ~6 x 10^7 bubbles/min, respectively (Figures 3b-e). Smaller (D_i = 1 - 2 μm) DEE-infused C_5F_{12} bubbles with *CV*s < 5 % were generated, but the monodispersity of these DEE-infused C_5F_{12} bubbles could not be maintained for extended periods (more than a few minutes) due to the fluctuation of the stepping motor of the syringe pump used in this MFD.[22] The minimum size of monodisperse DEE-infused PFC precursor bubbles produced at the highest DEE concentration will determine the smallest final PFC droplet size that can be formed using this MFD. Here, the minimum bubble size was close to 4.3 μm at Q_c = 1.7, Q_d = 0.04 mL/h, and ϕ_{C5F12} = 0.015.

DEE was selected as the cosolvent in these experiments due to its low b.p. (34.6 °C), its complete miscibility with the dispersed phases of C_5F_{12} or C_6F_{14} at 7 and 14 °C, respectively,[12, 23] and its limited solubility with the aqueous continuous phase (i.e., 9 vol. % at room temperature), which permit its controlled dissolution from the generated bubble. In addition, the relatively high vapour pressure of DEE permits its easy removal from the system after its dissolution from the precursor bubble. Furthermore, DEE decreases the viscosity of the dispersed PFC phase and the interfacial tension between the dispersed and continuous phases, facilitating the generation of smaller-sized precursor microbubbles at the MFD orifice. Since the size of the final PFC droplets are proportional to the size of the bubbles generated in the MFD, this last advantage of small bubble generation assisted in producing the smallest size droplets after condensation and cosolvent dissolution took place.[24]

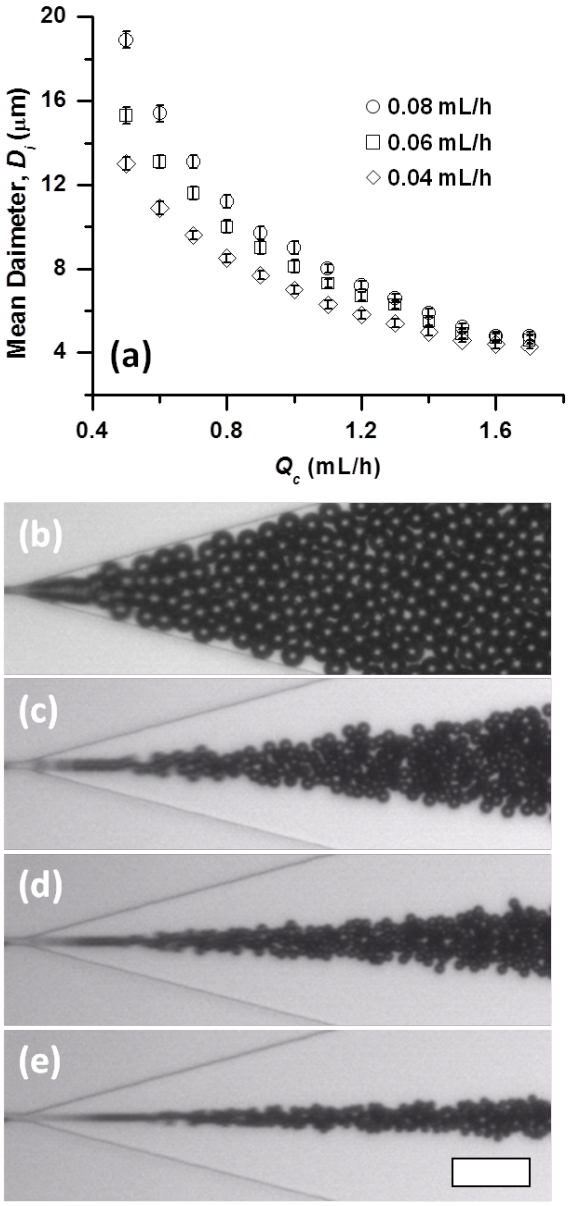

Figure 3. Generation of DEE-infused C_5F_{12} precursor bubbles: (a) Initial mean diameter (D_i) of the precursor bubbles produced in the MFD with different Q_c*s* and Q_ds. Microscope images show the generation of DEE-infused C_5F_{12} bubbles at Q_d = 0.08 mL/h and (b) Q_c = 0.6 mL/h (D_i = 15.4 μm); (c) Q_c = 0.9 mL/h (D_i = 9.7 μm); (d) Q_c = 1.3 mL/h (D_i = 6.6 μm); and (e) Q_c = 1.7 mL/h (D_i = 4.7μm). The volume fractions of C_5F_{12} and DEE in the starting liquid mixture were ϕ_{C5F12} = 0.015, and ϕ_{DEE} = 0.985, respectively. The MFD temperature was 45 °C, the height 25 μm, the width of the orifice was 6 μm, and the width of the downstream outer channel was 250 μm. The scale bar is 50 μm.

2. Formation of ultra-small PFC droplets *via* condensation and dissolution of DEE-infused PFC precursor bubbles

After generation of the DEE-infused PFC bubbles, the bubbles condensed to form droplets while DEE simultaneously diffused from the condensing bubbles to the aqueous continuous phase. To optically quantify the size reduction of the initial monodisperse DEE-infused PFC bubbles and the final pure PFC droplets, relatively large precursor bubbles (i.e., up to 100 μm in size) were generated (Figure 4). Since micron-scale droplets have low thermal stability compared to nanoscale droplets and can spontaneously form bubbles at room temperature,[7] a higher b.p. PFC (i.e., C_6F_{14}) was used to form bubbles that were more stable during optical characterization of the droplet formation process. The full condensation of and total DEE removal from the bubbles containing $\phi_{C6F14} = 0.014$ ($D_i = 99.1$ μm, $CV = 2.4$ %) resulted in pure C_6F_{14} droplets ($D_f = 4.2$ μm, $CV = 3.9$ %) that retained the narrow size distribution of the precursor bubbles. To the best of our knowledge, the size-change ratio (D_i/D_f) we observed due to the combined DEE dissolution and condensation of the DEE-infused C_6F_{14} bubble was the highest reported, with a value of 24.1 ± 1.3. This measured size-change ratio is close to the product of the size-change ratios due to DEE dissolution from DEE-infused C_6F_{14} droplets alone ($D_i/D_f = 4.2$) and the condensation of C_6F_{14} gas bubbles to droplets alone ($D_i/D_f = 5.0$).

The size change ratio (D_i/D_f) between the final PFC droplets and the precursor DEE-infused PFC bubbles as a function of the volume fraction of PFC in the starting liquid mixture was characterized for two different PFCs (Figure 5). No substantial difference in size reduction from bubbles to droplets between C_5F_{12} and C_6F_{14} was observed. As expected, for both C_5F_{12} and C_6F_{14} bubbles generated at $T_o = 45$ and 80 °C, respectively, the change in size from DEE-infused PFC bubbles to pure PFC droplets (D_i/D_f) correlated with the volume fraction of PFC in the initial starting liquid DEE-PFC mixture (ϕ_{PFC}), determined to be $D_i/D_f\,(T_o) = 4.97 \times \phi_{PFC}^{-0.367}$ ($R^2 = 0.996$) for bubbles formed at either T_o of 45 and 80 °C for C_5F_{12} and C_6F_{14}, respectively. Although D_i/D_f (i.e., $(V_i/V_f)^{1/3}$) are expected to scale with $\phi_{PFC}^{-1/3}$, slightly larger size changes were observed at low ϕ_{PFC} values. This is likely due to the greater volume expansion of DEE compared to PFC at a given T_o. Since the temperature range we are measuring is fairly low, the

similarity between the observed size change ratio between C_5F_{12} (where bubbles were produced 16 °C above its b.p.) and C_6F_{14} (where bubbles were produced 23°C above its b.p.) suggests the relationship between D_i/D_f has a much weaker dependence on T_o compared to its dependence on the volume fraction of PFC through this temperature range.

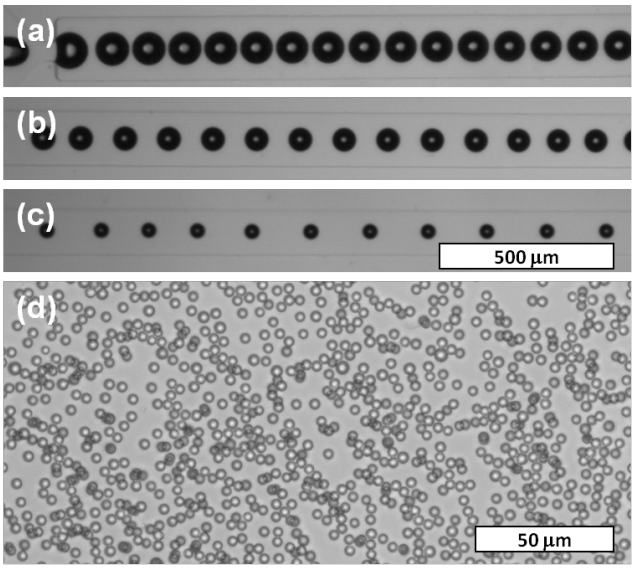

Figure 4. Formation of size-reduced C_6F_{14} droplets (D_f = 4.2 μm, CV = 3.9 %) after combined condensation and DEE dissolution from DEE-infused C_6F_{14} bubbles (D_i = 99.1 μm, CV = 2.4 %). Optical microscope images of DEE-infused C_6F_{14} bubbles in the MFD (T_o = 80 °C, Q_c = 7.0 mL/hr, Q_d = 0.04 mL/hr, ϕ_{C6F14} = 0.014): (a) at the orifice immediately after generation; (b) 9 mm downstream from the orifice; and (c) 20 mm downstream from the orifice. (d) Microscope image of the final droplets (D_f = 4.2 μm, CV = 3.9 %) after complete condensation and DEE dissolution from the precursor DEE-infused C_6F_{14} bubbles.

The maximum size-change ratio that we observed resulted from bubbles formed using starting volume fractions of ϕ_{C5F12} = 0.015 for C_5F_{12} and ϕ_{C6F14} = 0.014 for C_6F_{14} with the remainder of the dispersed phase made up of DEE. Under these conditions, the combined PFC condensation and DEE dissolution from the bubbles resulted in final PFC droplet diameters of 22.5 ± 1.5 and 24.1 ± 1.3 times smaller than the initial bubbles for

C_5F_{12} and C_6F_{14}, respectively. This corresponds to sizes 5.6 and 5.7 times smaller than the droplets generated from DEE dissolution alone from DEE-infused C_5F_{12} and C_6F_{14} droplets, respectively, using equivalent MFDs (Figure 5, $\phi_{PFC} = 1$).

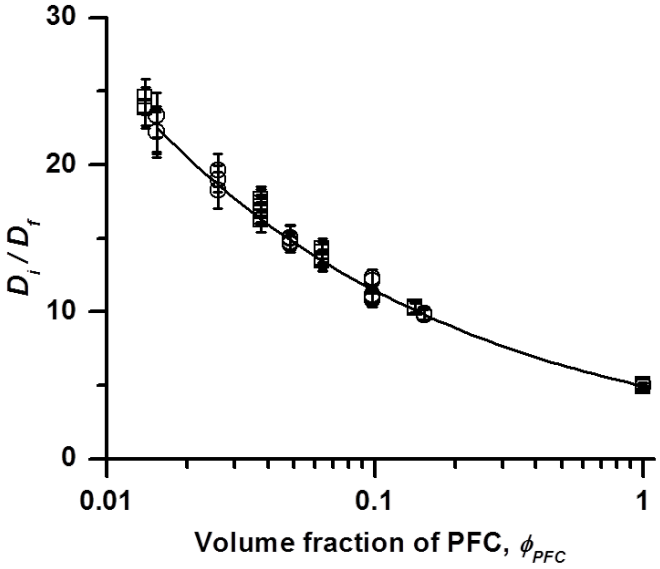

Figure 5. Size-change ratios (D_i/D_f) of DEE-infused PFC bubbles and final PFC droplets as a function of PFC volume fraction (ϕ_{PFC}) in the initial liquid mixture. DEE-infused C_5F_{12} (circle) and C_6F_{14} (square) bubbles were generated at 45 °C and at 80 °C, respectively. The best fit line is shown here as the solid line.

The minimum size-change ratio we observed resulted from bubbles made with pure PFC ($\phi_{PFC} = 1$). Here, the size change to droplets occurred purely by condensation (i.e., no dissolution) as shown in Figure 6. Pure condensation results in D_i/D_f of 5.0 ± 0.1 times for C_5F_{12} (T_o = 45 °C), and D_i/D_f of 4.9 ± 0.1 times for C_6F_{14} (T_o = 80 °C). This differs slightly from the theoretically predicted diameter change of 5.2 and 5.1 times for C_5F_{12} and C_6F_{14}, respectively,[14, 25] at atmospheric pressure. This discrepancy is attributed to the fact that the pressure inside of the microchannel is higher than atmospheric pressure because of the confined geometry of the microchannel, the heating of the MFD, and the fluid flow.

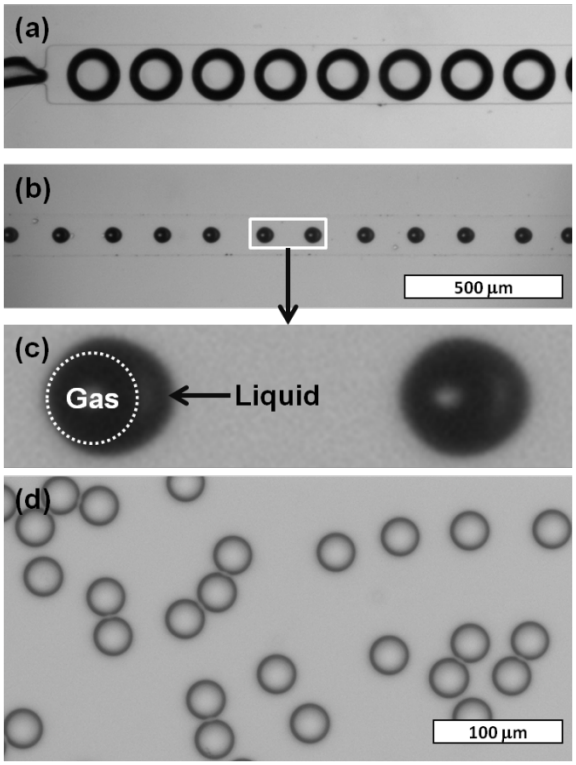

Figure 6. Microscope images of the condensation of pure C_6F_{14} bubbles into PFC droplets (T_o = 80 °C, Q_c = 2.0 mL/hr, Q_d = 0.05 mL/hr): (a) near the MFD orifice (D_i = 154.7 μm, CV = 2.4 %), (b) 19 mm downstream from the orifice, (c) magnified view of the condensing C_6F_{14} bubbles containing both gas and liquid phases (the white broken line indicates the location of the gas phase), and (d) fully condensed droplets in the collector (D_f = 31.4 μm, CV = 2.6 %).

It should be noted that the initial volume fraction of PFC in the liquid phase (ϕ_{PFC}) is not equivalent to the volume fraction of PFC in the gas bubble formed at the MFD orifice. This is due to the fact that the temperature-dependent volume expansion from liquid to gas differs between DEE and PFC. The volume expansion ratio ($\propto (D_i/D_f)^3$) of DEE was found to be 179 ± 4 times (R^2 = 0.99) at 45 °C, and 199 ± 3 times at 80 °C (R^2 = 0.99) (Supplementary Information). The theoretical volume expansion ratios of DEE at 45 °C and 80 °C in this MFD is 214 and 222 times, respectively.[14, 25] The discrepancy between the measured and theoretical values may have resulted from the fact that there may be mixing of the PFC gas and the DEE gas such that the initial volumes of

the DEE-infused PFC bubbles are slightly smaller than the sum of the individual volumes of each solvent.[26]

We have found that the combined effects of condensation and cosolvent dissolution can transform DEE-infused PFC bubbles into droplets below the micron-scale and well below the smallest sizes of regular droplet formation of an MFD. For example, we produced nanoscale C_5F_{12} droplets using condensation and DEE dissolution of DEE-infused C_5F_{12} bubbles ($\phi_{C5F12} = 0.015$) with initial diameters ranging from 5 μm to 20 μm (Figure 7). In this experiment, monodisperse C_5F_{12} nanodroplets with average mean diameters of 240, 460, and 870 nm were generated from DEE-infused C_5F_{12} bubbles ($\phi_{C5F12} = 0.015$) with corresponding original sizes of 4.8, 9.7 and 18.9 μm, respectively, and with narrow size distribution of the polydispersity indices of the droplets between 0.02 and 0.05.

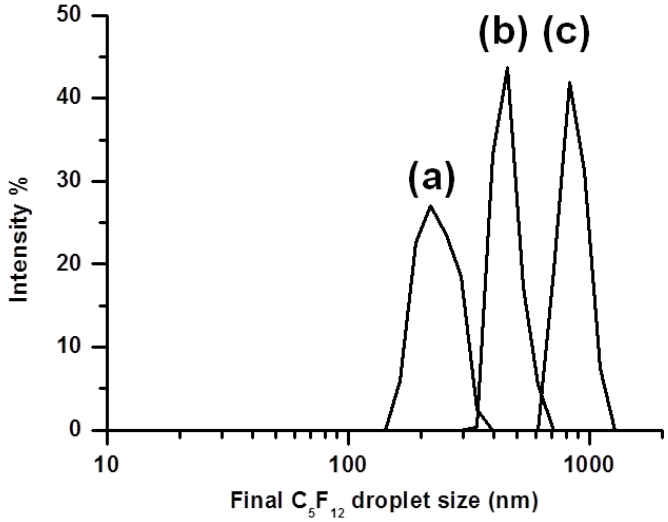

Figure 7. Size distribution of pure C_5F_{12} nanoscale droplets after condensation and dissolution of DEE from DEE-infused bubbles: (a) D_f = 240 nm (Polydispersity index, PDI = 0.04), from precursor bubbles with D_i = 4.8 μm (CV = 3.6 %), (b) D_f = 460 nm (PDI = 0.04), from precursor bubbles with D_i = 9.7 μm (CV = 2.9 %), and (c) D_f = 870 nm (PDI = 0.02), from precursor bubbles with D_i = 18.9 μm (CV = 2.3 %). All precursor bubbles were made using C_5F_{12} volume fractions of $\phi_{C5F12} = 0.015$.

Furthermore, this combined condensation and cosolvent dissolution approach was found to retain the low *CV*s of the precursor bubbles in the final droplets. In previous studies, we found the dissolution of high concentrations of cosolvent into the continuous phase generated satellite droplets from formation of multiple nucleation points of the undissolved dispersed phase.[12, 27] We did not observe the formation of satellite droplets in this approach. We believe that this is due to the droplets being generated in the gas phase, which provides higher mobility of the molecules and higher interfacial tension between the bubbles and the continuous phase than when droplets are generated in the liquid phase. Both of these properties together allow the kinetic reorganization of the molecules within the bubbles to prevent multiple nucleation points within a single bubble on condensation and cosolvent dissolution.

In general, appropriate cosolvents require a boiling point lower than the melting points of the shell materials, miscibility with PFCs at temperatures lower than those that would affect the MFD and/or shell materials, low reactivity with the shell materials, water solubility so that the cosolvent can be controllably removed from the bubble and droplet, and a means by which to remove it from the aqueous phase (e.g., relatively high cosolvent vapour pressure). For the synthesis of C_5F_{12} or C_6F_{14} droplets stabilized with fluorosurfactants and synthesized using the PDMS microfluidic system used here, to the best of our knowledge, DEE was the most suitable cosolvent for this study. However, this approach should be easily transferable to other material systems, including low b.p. hydrocarbons, such as pentane (b.p.: 36.1 °C), cyclopentane (b.p.: 40 °C), and hexane (b.p.: 68 °C), in combination with other properly chosen cosolvents.

3. Ultrasound characterization of nanoscale PFC droplets

Liquid PFC droplets can be vapourized to form highly echogenic bubbles *in situ* following high-pressure ultrasound exposure. Indeed, nanoscale C_5F_{12} droplets (D_f = 320 nm) loaded in PAA gel were successfully converted into echogenic bubbles after exposure to ultrasound at 37 °C (Figure 8a and 8b). (A movie of nanoscale PFC droplets imaged using low-power ultrasound before, during, and after their conversion to bubbles is available in the Supplementary Information). Before high-pressure ultrasound exposure, no bubbles were observed in the PAA gel using low-pressure ultrasound imaging. During

the high-pressure ultrasound exposure of the droplets, the droplets were converted to echogenic bubbles that were clearly imaged after the high-pressure exposure throughout the gel using low-power ultrasound imaging (Figure 8c).

Microscopy of the bubbles after ultrasound-induced conversion (Figures 8d and 8e) indicated that the echogenic bubbles were monodisperse. The size increase from liquid droplet to gas bubble after ultrasound exposure was observed to be larger (D_{bubble}/D_f = 5.7 to 7.7) than the size decrease due to condensation of pure C_5F_{12} bubbles to C_5F_{12} droplets (D_f/D_i = 5.0). The growth of bubbles over time after ultrasound conversion to bubbles has been previously observed and is due to the intake of dissolved gases from the surrounding fluid after conversion of PFC droplets to gas bubbles.[14, 28, 29] This is an expected effect because although the PAA gel solution was degassed, the OptiCell® has two parallel gas-permeable membranes with surface area *ca.* 100 cm^2.

After high-pressure ultrasound exposure, a number of unconverted PFC droplets were observed (e.g., as shown in Figure 8d). Not all droplets vapourize under these brief ultrasound exposure times because vapourization depends on the occurrence of nucleation within the droplet, which has an increased statistical chance of occurring under longer or higher pressure ultrasound exposure. Furthermore, it has been demonstrated that for polydisperse submicron droplets, a significant number that undergo vapourization will recondense within a few microseconds and some may also undergo coalescence during vapourization.[29] The vapourization efficiency was further investigated using larger C_5F_{12} droplets (Figure 9a). After exposure to high-pressure ultrasound, some of the droplets are clearly converted to bubbles (Figure 9b), and the bubbles formed by ultrasound-induced droplet vapourization are monodisperse (CV = 3.5 %). The size increase ratio we observed from C_5F_{12} droplet to gas bubble (D_{bubble}/D_f) after 4 minutes of high-pressure ultrasound exposure was 7.9.

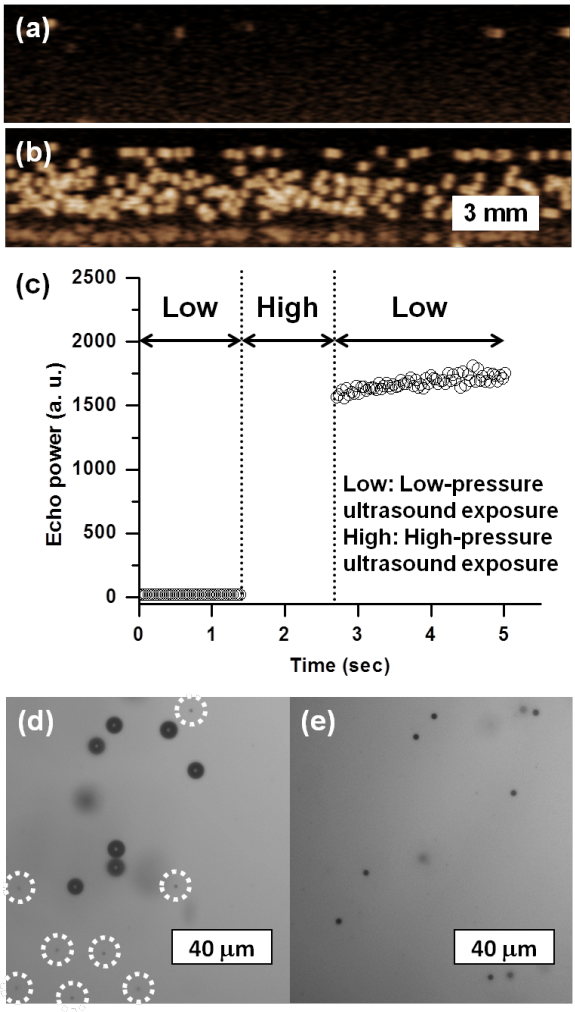

Figure 8. *In vitro* ultrasound images of an Opticell® (in cross-section), filled with C_5F_{12} droplets (a) before and (b) after the conversion to bubbles by ultrasound exposure. (c) The strength of the echo power change before and after the high-pressure ultrasound exposure of 320 nm C_5F_{12} droplets loaded in PAA gel at 37 °C. Time-series data were collected from the movie provided in the Supplementary Information. Microscope images of the bubbles formed from two different sizes of PFC droplets after ultrasound exposure: (d) Droplets (D_f = 1.3 μm) were vapourized to form bubbles of diameter 7.1 μm, captured 2 minutes after droplet vapourization. The white dashed circles indicate the location of the unconverted C_5F_{12} droplets. (e) Droplets (D_f = 0.3 μm) were vapourized to form bubbles of diameter 2.4 μm, captured 4 minutes after droplet vapourization.

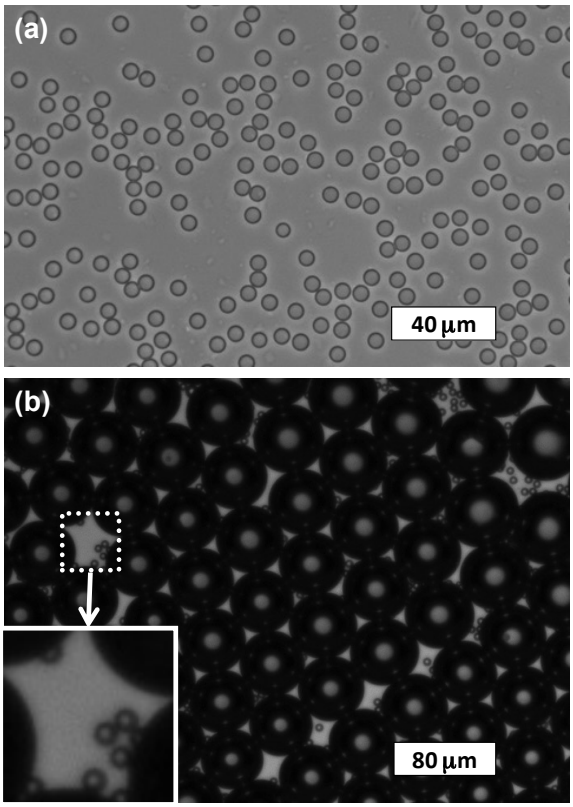

Figure 9. (a) Microscope image of C_5F_{12} droplets (D_f = 6.6 μm, CV = 2.7 %) on the glass slide after complete condensation and DEE dissolution from the precursor DEE-infused C_5F_{12} bubbles. (b) Microscope images of C_5F_{12} droplets and bubbles (D_{bubble} = 52.4 μm, CV = 3.5 %) embedded in PAA gel after exposure to high-pressure ultrasound, showing the monodispersity of both the converted bubbles and the unconverted droplets. The image was taken 4 minutes after high-pressure ultrasound exposure.

Phase-change droplets are applicable to drug delivery, ultrasound therapeutic ablation, embolotherapy, and tumour imaging. Since the vaporization threshold is strongly size dependent, monodisperse droplets permit the fine-tuning of exposure parameters due to their uniformity of response in comparison with polydisperse populations, while ensuring that unwanted vapourization events are minimal. In a polydisperse droplet delivery system, many droplets will be too small to vapourize at a given pressure or so large as to risk occluding vessels or to cause unwanted bioeffects at low ultrasound pressures. Monodisperse droplets can statistically reduce the unwanted vaporization of large droplets at low pressures, which is particularly important in

therapeutic applications. For drug delivery, by injecting fewer small droplets that would be unlikely to vaporize at standard diagnostic ultrasound pressures, the therapeutic ratio would be enhanced due to a decreased dose required to achieve the same effect as with polydisperse droplets.

Conclusion

Monodisperse PFC droplets were formed through size reduction by the condensation and dissolution of MFD-generated, DEE-infused PFC bubbles. The combination of condensation and cosolvent dissolution of DEE-infused PFC bubbles resulted in final monodisperse droplets down to 240 nm in size, with diameters 24 times smaller than the precursor bubbles (ϕ_{PFC} = 0.014 and ϕ_{DEE} = 0.986). This size reduction was substantially smaller than that achieved by using either bubble condensation alone (5.7 times size reduction) or cosolvent dissolution alone at the same DEE concentration (4.2 times size reduction). The production of these droplets suggests that standard MFDs can form nanoscale PFC droplets that are suitable as injectable phase-change contrast agents for ultrasound imaging. The final monodisperse PFC droplets were converted to echogenic monodisperse bubbles upon exposure to ultrasound, demonstrating the potential relevance of these droplets as new size-controlled agents to medical imaging and therapy applications.

Acknowledgments

This project was funded, in part, by the Ontario Institute for Cancer Research Network through funding provided by the Province of Ontario, the Ontario Research Fund-Research Excellence Program and the Early Researcher Award – ER14-10-178, the Cancer Imaging Network of Ontario (CINO) supported by Cancer Care Ontario with funds from the Ministry of Health and Long-Term Care, an award by Prostate Cancer Canada, proudly funded by the Movember Foundation – Grant # D2014-7, a grant from the Fight Against Cancer Innovation Trust (FACIT), and the NSERC Discovery Grants Program – RGPIN-2015-05835. The authors thank Drs. P. S. Sheeran and Selva Nair for useful scientific discussions, and acknowledge material support from Drs. P. N. Burns, F. S. Foster, and J. A. Rowlands.

References

1. Riess, J. G., Oxygen carriers ("blood substitutes") - Raison d'Etre, chemistry, and some physiology. *Chem. Rev.* **2001,** 101, (9), 2797-2919.
2. Schutt, E. G.; Klein, D. H.; Mattrey, R. M.; Riess, J. G., Injectable microbubbles as contrast agents for diagnostic ultrasound imaging: The key role of perfluorochemicals. *Angew. Chem. Int. Ed.* **2003,** 42, (28), 3218-3235.
3. Jain, R. K.; Stylianopoulos, T., Delivering nanomedicine to solid tumors. *Nat. Rev. Clin. Oncol.* **2010,** 7, (11), 653-664.
4. Yuan, F.; Dellian, M.; Fukumura, D.; Leunig, M.; Berk, D. A.; Torchilin, V. P.; Jain, R. K., Vascular-Permeability in a Human Tumor Xenograft - Molecular-Size Dependence and Cutoff Size. *Cancer Res.* **1995,** 55, (17), 3752-3756.
5. Maeda, H.; Wu, J.; Sawa, T.; Matsumura, Y.; Hori, K., Tumor vascular permeability and the EPR effect in macromolecular therapeutics: a review. *J. Control. Release* **2000,** 65, (1-2), 271-284.
6. Matsuura, N.; Rowlands, J. A., Towards new functional nanostructures for medical imaging. *Med. Phys.* **2008,** 35, (10), 4474-4487.
7. Martin, A. L.; Seo, M.; Williams, R.; Belayneh, G.; Foster, F. S.; Matsuura, N., Intracellular Growth of Nanoscale Perfluorocarbon Droplets for Enhanced Ultrasound-Induced Phase-Change Conversion. *Ultrasound Med. Biol.* **2012,** 38, (10), 1799-1810.
8. Teh, S. Y.; Lin, R.; Hung, L. H.; Lee, A. P., Droplet microfluidics. *Lab Chip* **2008,** 8, (2), 198-220.
9. Martz, T. D.; Bardin, D.; Sheeran, P. S.; Lee, A. P.; Dayton, P. A., Microfluidic Generation of Acoustically Active Nanodroplets. *Small* **2012,** 8, (12), 1876-1879.
10. Anna, S. L.; Mayer, H. C., Microscale tipstreaming in a microfluidic flow focusing device. *Phys. Fluids* **2006,** 18, (12), 121512.
11. Christopher, G. F.; Anna, S. L., Microfluidic methods for generating continuous droplet streams. *J. Phys. D: Appl. Phys.* **2007,** 40, (19), R319-R336.
12. Seo, M.; Matsuura, N., Direct Incorporation of Lipophilic Nanoparticles into Monodisperse Perfluorocarbon Nanodroplets via Solvent Dissolution from Microfluidic-Generated Precursor Microdroplets. *Langmuir* **2014,** 30, (42), 12465-12473.
13. Seo, M.; Matsuura, N., Monodisperse, Submicrometer Droplets via Condensation of Microfluidic-Generated Gas Bubbles. *Small* **2012,** 8, (17), 2704-2714.
14. Sheeran, P. S.; Wong, V. P.; Luois, S.; McFarland, R. J.; Ross, W. D.; Feingold, S.; Matsunaga, T. O.; Dayton, P. A., Decafluorobutane as a Phase-Change Contrast Agent for Low-Energy Extravascular Ultrasonic Imaging. *Ultrasound Med. Biol.* **2011,** 37, (9), 1518-1530.
15. Williams, R.; Wright, C.; Cherin, E.; Reznik, N.; Lee, M.; Gorelikov, I.; Foster, F. S.; Matsuura, N.; Burns, P. N., Characterization of Submicron Phase-Change Perfluorocarbon Droplets for Extravascular Ultrasound Imaging of Cancer. *Ultrasound Med. Biol.* **2013,** 39, (3), 475-489.
16. Gorelikov, I.; Martin, A. L.; Seo, M.; Matsuura, N., Silica-Coated Quantum Dots for Optical Evaluation of Perfluorocarbon Droplet Interactions with Cells. *Langmuir* **2011,** 27, (24), 15024-15033.

17. Xia, Y. N.; Whitesides, G. M., Soft lithography. *Angew. Chem. Int. Ed.* **1998,** 37, (5), 551-575.
18. Wang, K.; Xie, L. S.; Lu, Y. C.; Luo, G. S., Generation of monodispersed microdroplets by temperature controlled bubble condensation processes. *Lab Chip* **2013,** 13, (1), 73-76.
19. Wu, D. P.; Luo, Y.; Zhou, X. M.; Dai, Z. P.; Lin, B. C., Multilayer poly(vinyl alcohol)-adsorbed coating on poly(dimethylsiloxane) microfluidic chips for biopolymer separation. *Electrophoresis* **2005,** 26, (1), 211-218.
20. McDonald, M.; Lochhead, S.; Chopra, R.; Bronskill, M. J., Multi-modality tissue-mimicking phantom for thermal therapy. *Phys. Med. Biol.* **2004,** 49, (13), 2767-2778.
21. NIST, Measuring the Size of Nanoparticles in Aqueous Media Using Batch-Mode Dynamic Light Scattering, NCL Joint Assay Protocol. In *NCL Joint Assay Protocol*, National Institute of Standards and Technology: February 2010.
22. Korczyk, P. M.; Cybulski, O.; Makulska, S.; Garstecki, P., Effects of unsteadiness of the rates of flow on the dynamics of formation of droplets in microfluidic systems. *Lab Chip* **2011,** 11, (1), 173-175.
23. Babiak, P.; Nemcova, A.; Rulisek, L.; Beier, P., On the miscibility of ethers and perfluorocarbons an experimental and theoretical study. *J. Fluorine Chem.* **2008,** 129, (5), 397-401.
24. Nishikido, N.; Mahler, W.; Mukerjee, P., Interfacial-Tensions of Perfluorohexane and Perfluorodecalin against Water. *Langmuir* **1989,** 5, (1), 227-229.
25. Rapoport, N. Y.; Kennedy, A. M.; Shea, J. E.; Scaife, C. L.; Nam, K.-H., Controlled and targeted tumor chemotherapy by ultrasound-activated nanoemulsions/microbubbles. *J. Control. Release* **2009,** 138, (3), 268-276.
26. Lepori, L.; Matteoli, E.; Spanedda, A.; Duce, C.; Tine, M. R., Volume changes on mixing perfluoroalkanes with alkanes or ethers at 298.15 K. *Fluid Phase Equilib.* **2002,** 201, (1), 119-134.
27. Shum, H. C.; Lee, D.; Yoon, I.; Kodger, T.; Weitz, D. A., Double emulsion templated monodisperse phospholipid vesicles. *Langmuir* **2008,** 24, (15), 7651-7653.
28. Bardin, D.; Martz, T. D.; Sheeran, P. S.; Shih, R.; Dayton, P. A.; Lee, A. P., High-speed, clinical-scale microfluidic generation of stable phase-change droplets for gas embolotherapy. *Lab Chip* **2011,** 11, (23), 3990-3998.
29. Reznik, N.; Seo, M.; Williams, R.; Bolewska-Pedyczak, E.; Lee, M.; Matsuura, N.; Gariepy, J.; Foster, F. S.; Burns, P. N., Optical studies of vaporization and stability of fluorescently labelled perfluorocarbon droplets. *Phys. Med. Biol.* **2012,** 57, (21), 7205-7217.